Two-Dimensional Modeling of Ion Implantation Induced Point Defects

GERHARD HOBLER, STUDENT MEMBER, IEEE, AND SIEGFRIED SELBERHERR, SENIOR MEMBER, IEEE

***Abstract*—We present an analytical model for the description of ion implantation induced damage profiles. The model is based on extensive Monte Carlo simulations of B-, P-, As-, and Sb-implantations in Si. One-dimensional profiles are described by a Gaussian function and an exponential function joined together continuously with continuous first derivatives. The two-dimensional model has previously been developed by the authors for dopant profiles and is demonstrated to apply well to point defect distributions. Parameters have been obtained for the four ions by fitting the model to the Monte Carlo results, and they are provided by tables for the energy range of 10–300 keV (for the 1D model 1–300 keV). The Monte Carlo simulations are based on the binary collision approximation, the assumption of a random target, and the validity of the linear collision cascade theory. We point out the importance of energy transport by recoils.**

I. Introduction

The strong influence of point defects on the diffusion behavior of dopants in silicon is well known, and is taken into account in today's simulation programs. A good example is oxidation enhanced diffusion: It has been shown [1] that enhanced diffusion of dopants during thermal oxidation is caused by the generation of interstitials at the oxide–silicon interface. There is general agreement that adequate simulation of oxidation enhanced diffusion requires the solution of diffusion equations for the point defects [2], [3].

On the other hand, it is known that a great amount of defects is produced during ion implantation. However, no attempt has been made until now to consider these defects in diffusion programs in order to study their influence on the subsequent annealing process. In fact, there is experimental evidence that—in the case of boron implantations in silicon—diffusion is enhanced during the initial stage of rapid thermal annealing, and there are strong indications that the enhancement is due to implantation damage [4]. (It should be noted that the situation is not so clear for other ion species like arsenic [5].)

There are various approaches to calculate the spatial distribution of point defects [6]–[10], which are based on the so-called collision cascade model: In close collisions, the ions set target atoms into motion, which travel some distance in the target (they are called "recoils"). On their way, they may generate other recoils, these may again generate recoils and so on. It is assumed that the recoils leave behind a vacancy when they are produced, and form an interstitial when they come to rest.

However, introducing damage profiles from one of the theories [6]–[10] into diffusion programs, one will probably face some difficulties. The main problem is that these theories give no information, whether the displaced atoms form separated point defects or cluster to extended defects. Experiments and theoretical considerations indicate that light ions mainly produce point defects, whereas heavy ions produce small amorphous zones along their paths [11], [12]. In the case of extended defects one should know, how they dissolve and emit point defects during the annealing process.

Another problem is that absolute defect concentrations are not very well predicted by the collision cascade model. One reason is that temperature is ignored by theory, although it has been observed that defect production is reduced by a factor of about 10 at room temperature as compared with, say, 77 K [13]. On the other side, this is partly outweighed for heavy ions by an underestimate of defects at low temperature, which is thought to be due to nonlinearities in connection with the formation of amorphous zones along the ion paths [12]. In any case, one cannot expect from theory defect concentrations with an accuracy better than an order of magnitude.

In contrast, theories predict well the range of damage, even in two dimensions. This has been shown by Krimmel *et al.* [14], who investigated the two-dimensional damage distribution near a mask edge by transmission electron microscopy and found good agreement with the theoretical predictions of Matsumura and Furukawa [7].

In spite of the difficulties mentioned above, a simple and accurate description of defect distributions as they are obtained by the present theories is certainly useful for further investigations. Moreover, apart from the challenging task of explaining anomalous diffusion during rapid thermal annealing, there is still the "traditional" application of predicting the range of amorphous zones for high-dose implantations. The practical relevance of this problem arises from the fact that after regrowth of the amorphous layer heavy damage remains at the former amorphous/crystalline interface. So it is important that this interface

Manuscript received March 17, 1987; revised July 27, 1987. This work was supported by the research laboratories of SIEMENS AG., Munich, Germany, by Digital Equipment Corporation, Hudson, NY, and by Fönds zur Forderung der wissenschaftlichen Forschung, under Project S43/10. The review of this paper was arranged by R. W. Dutton.

The authors are with the Institut für Allgemeine Elektrotechnik und Elektronik, Technical University of Vienna, A-1040 Vienna, Austria.

IEEE Log Number 8717572.

0278-0070/88/0200-0174$01.00 © 1988 IEEE

is not located in a critical region of the later semiconductor device [15].

We will continue in Section II with a description of the Monte Carlo simulation of defect production. In particular we point out the importance of the finite range of the recoils for the case of heavy ions. This has been known in principle for a long time, but is still sometimes neglected for the sake of saving computer time [16]. In Section III a simple and very accurate analytical model to describe the Monte Carlo distributions is presented. The two-dimensional model has actually been developed for dopant profiles [17], but it turned out to be perfectly suited to describe also point defect distributions with their great variation of lateral standard deviation and sometimes large values of lateral kurtosis. All parameters of the model will be given by tables, for the ions boron, phosphorus, arsenic, and antimony implanted in silicon, for energies up to 300 keV.

II. Monte Carlo Simulation

Implantation damage has traditionally been calculated by approaches similar to LSS-Theory (e.g., [6]), by solving Boltzmann Transport Equations [8], or by Monte Carlo method [9], [10]. We have chosen the Monte Carlo method, because it is the most flexible and accurate approach, although it requires large computer times.

In the Monte Carlo approach a large number of ion trajectories is simulated, and the dopant profile is made up by the end points of the trajectories. For calculating defect distributions, the recoil motion may be simulated just in the same way. A recoil is assumed to be generated, if the incoming atom transfers an energy to the target atom which is greater than the displacement energy E_d = 15 eV. A vacancy is produced at the location of the collision, unless the energy of the incoming atom drops below the displacement energy. In this case the incoming atom is assumed to replace the recoiled atom. Analogously, an interstitial is produced at the end of the recoil trajectory, unless it ends up in a replacement collision. The calculation procedure is similar to that of the program "TRIM.CASC" as described in [10]. The only (slight) difference is the treatment of the end of the recoil trajectories. In [10] the trajectory is terminated, if the recoil energy drops below a value $E_{\min}$, which corresponds to a mean recoil range less than the grid spacing of the calculated histogram. The number of point defects N_{vac} which would be produced on the remaining part of the trajectory is calculated by the modified Kinchin-Pease model and recorded at the point where the recoil has dropped below $E_{\min}$. In contrast, we have precalculated the mean damage range $R_p(E)$ and the number of point defects $N_{\text{vac}}(E)$ as a function of energy by Monte Carlo method (with $E_{\min} = E_d$), and record the number of point defects N_{vac} at a distance R_p from the location where the recoil energy has dropped below $E_{\min}$. Concerning physical parameters for nuclear and electronic stopping, we refer to our previous paper [17].

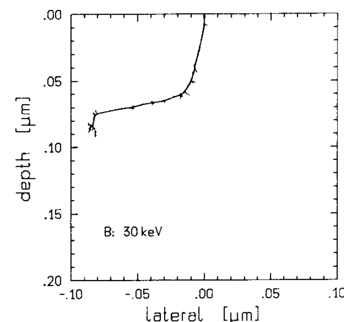

Fig. 1. Simulated trajectories of a boron ion (bolt line) and of all recoils with energies above 100 eV (thin lines). Implantation energy: 30 keV.

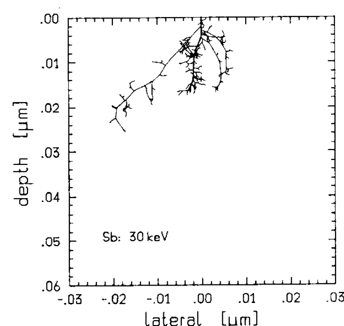

Fig. 2. Simulated trajectories of an antimony ion (bolt line) and of all recoils with energies above 100 eV (thin lines). Implantation energy: 30 keV.

Considering that every ion produces on the order of 100 to 1000 recoils, one can imagine that detailed simulation of collision cascades takes a lot of computer time. For that reason, in some codes [16] the recoils are not followed explicitly. Instead, the modified Kinchin–Pease model [18]–[20] is applied to the primary recoils, i.e., the number of point defects is calculated by an analytical formula from the energy transferred in the ion–target atom collision, and is recorded at the location of the collision.

Obviously, this is only justified, if the collision cascades are small. Figs. 1 and 2 show one simulated ion trajectory for the case of boron and antimony implantations in silicon, respectively (bolt lines), and all trajectories of recoils with energies above 100 eV (thin lines). It can be seen that collision cascades are very small in the case of boron (Fig. 1), so that Kinchin–Pease model may be applied. But the opposite is true for antimony (Fig. 2). In the left part of Fig. 2 a recoil can be seen which has even a greater range than the ion itself. Applying Kinchin–Pease model would mean that this recoil and all other recoils produced in this collision cascade would be recorded at the generation point of the primary recoil, which is obviously erroneous.

The impact on the one-dimensional damage profiles can be seen in Figs. 3 and 4, where profiles calculated by the modified Kinchin–Pease model and by detailed simulation

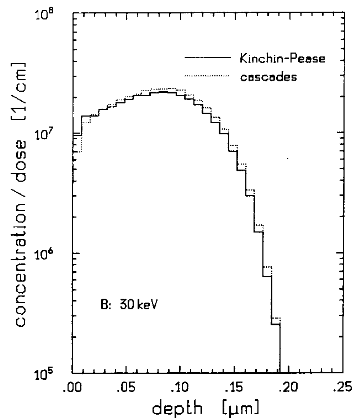

Fig. 3. Monte Carlo damage profiles due to Kinchin-Pease model (full line) and detailed simulation of collision cascades (dotted line). Boron implanted in silicon at 30 keV.

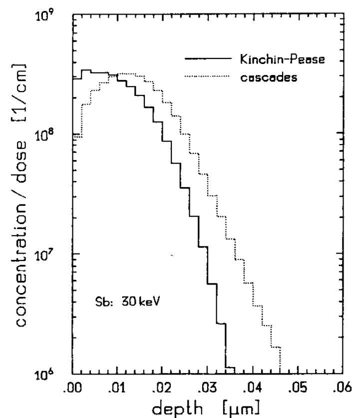

Fig. 4. Monte Carlo damage profiles due to Kinchin-Pease model (full line) and detailed simulation of collision cascades (dotted line). Antimony implanted in silicon at 30 keV.

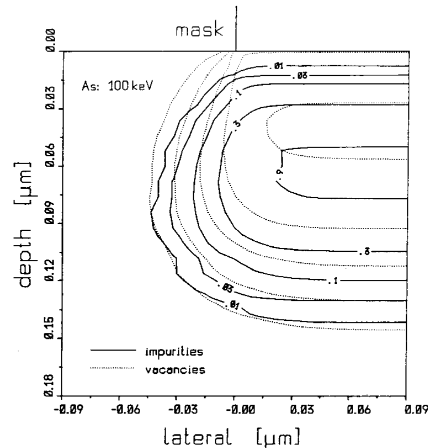

Fig. 5. Monte Carlo simulation of an arsenic implantation at 100 keV by a vertical mask edge, considering collision cascades. Contour lines for the dopant distribution (full lines) and for the point defect distribution (dotted lines).

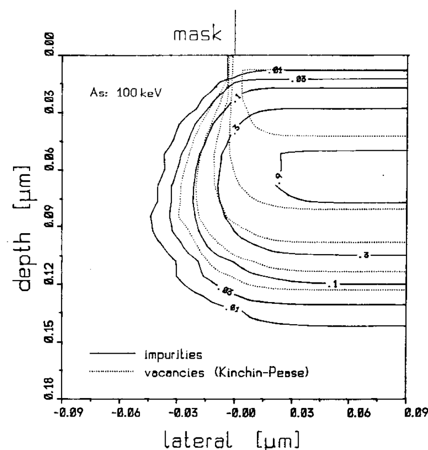

Fig. 6. Monte Carlo simulation of an arsenic implantation at 100 keV by a vertical mask edge, using Kinchin-Pease model. Contour lines for the dopant distribution (full lines) and of the point defect distribution (dotted lines).

of collision cascades are compared. As expected, the two profiles are very close to each other in the case of boron, but there is a great difference for antimony. In the latter case the profile has a long tail, which is caused by energy transport of recoils into the target. The same effect can be observed in the lateral direction. Figs. 5 and 6 show the dopant and the damage distribution (full lines and dotted lines, respectively) for an arsenic implantation by a vertical mask edge. In all cases the contour lines correspond to 0.9, 0.3, 0.1, 0.03, and 0.01 of the maximum concentration. The distribution due to Kinchin-Pease model (Fig. 6) does not only extend not far enough into the bulk, but also not far enough below the mask edge (cf. Fig. 5).

The error introduced by using the Kinchin-Pease model does not depend very much on the implantation energy, but it depends critically on the ion mass. For light ions such as boron (relative atomic mass $M = 11$) the ion range is large and the recoil range is small. For heavy ions, such as arsenic ($M = 75$) and antimony ($M = 121$), the ion range is small, and there are large collision cascades. Phosphorus ($M = 31$) lies somewhere between arsenic and boron, the error is roughly half as large as for arsenic.

Finally, we would like to mention that our code is capable of producing different profiles for vacancies and interstitials. One would expect that interstitial profiles are deeper than vacancy profiles, because recoils move mainly towards the bulk of the target. However, in histograms we have never observed any difference, and in the mean damage range there was only a very small difference: Interstitials are on an average only 1–2 Å deeper than vacancies. The reason is that in spite of few recoils which may travel a long distance in the target, most recoils have only a very small range.

III. Analytical Model

3.1. One-Dimensional Model

Analytical models for the description of one-dimensional profiles usually involve spatial moments. One criterion for these models is that the parameters for the analytical distribution function should be easily computed from the moments. For example, in the case of the widely used Pearson IV function the parameters may be calculated from the first four moments by simple analytical formulas. However, these formulas are derived under the assumption that the Pearson IV function describes the dopant concentration everywhere ($-\infty < z < +\infty$), i.e., also in the vacuum ($z < 0$). (z denotes the spatial coordinate perpendicular to the surface.) Since the dopant concentration is zero in the vacuum, the formulas are only valid, if the Pearson IV function is sufficiently small for $z < 0$. This is the case, if the dopant concentration at the surface is very small, what is usually true for dopant profiles.

Unfortunately, this is not true for point defect profiles (cf. Figs. 3, 4, 7, and 8). For this reason, a moments method seems not feasible. Instead, we propose the following model, which comprises a Gaussian function and an exponential function joined together continuously with continuous first derivatives ($f(z)$ denotes the point defect concentration as a function of depth).

- For the light ion species boron and phosphorus we take

$$f(z) = \begin{cases} C_1 \cdot \exp\left(\frac{z}{a_1}\right), & z \le z_0 \\ C_2 \cdot \exp\left[-\frac{(z-a_2)^2}{2 \cdot a_3^2}\right], & z \ge z_0 \end{cases} \tag{1}$$

The joining point z_0 is simply calculated by

$$z_0 = a_2 - \frac{a_3^2}{a_1}. \tag{2}$$

The parameters C_1 and C_2 can be evaluated analytically by

$$C_1 = N_d \cdot N_{\text{vac}} \cdot c_1 \tag{3a}$$

$$C_2 = N_d \cdot N_{\text{vac}} \cdot c_2 \tag{3b}$$

where N_d denotes the implantation dose and N_{vac} the number of point defects per ion. (This formula assumes that the damage concentration is proportional to the implantation dose, what is valid within the frame outlined in Section I, until the point defect concentration approaches the atomic density of the target.) c_1 and c_2 are given by

$$c_1 = \left\{a_1 \cdot \left[\exp\left(\frac{z_0}{a_1}\right) - 1\right] + a_3 \cdot \sqrt{\frac{\pi}{2}} \cdot \exp\left(\frac{z_1}{a_1}\right) \cdot \text{erfc}\left(\frac{z_0 - a_2}{\sqrt{2} \cdot a_3}\right)\right\}^{-1} \tag{4a}$$

$$c_2 = c_1 \cdot \exp\left(\frac{z_1}{a_1}\right) \tag{4b}$$

with

$$z_1 = a_2 - \frac{a_3^2}{2 \cdot a_1}. \tag{5}$$

- For arsenic and antimony the exponential tail is towards the bulk:

$$f(z) = \begin{cases} C_2 \cdot \exp\left[-\frac{(z-a_2)^2}{2 \cdot a_3^2}\right], & z \le z_0 \\ C_1 \cdot \exp\left(\frac{z}{a_1}\right), & z \ge z_0 \end{cases} \tag{6}$$

Equation (2)-(5) are still valid, except for (4), which is replaced by

$$c_2 = \left\{-a_1 \cdot \exp\left(\frac{z_0 - z_1}{a_1}\right) + a_3 \cdot \sqrt{\frac{\pi}{2}} \cdot \left[2 - \text{erfc}\left(\frac{a_2}{\sqrt{2} \cdot a_3}\right) - \text{erfc}\left(\frac{z_0 - a_2}{\sqrt{2} \cdot a_3}\right)\right]\right\}^{-1} \tag{7a}$$

$$c_1 = c_2 \cdot \exp\left(-\frac{z_1}{a_1}\right). \tag{7b}$$

- In some cases a single Gaussian function is best. Then c_2 is given by

$$c_2 = \left\{a_3 \cdot \sqrt{\frac{\pi}{2}} \cdot \text{erfc}\left(-\frac{a_2}{\sqrt{2} \cdot a_3}\right)\right\}^{-1}. \tag{8}$$

In this model the four parameters a_1, a_2, a_3, and N_{vac} are required, which correspond to the decay length of the exponential function, to peak position and standard deviation of the Gaussian function, and to the number of point defects per ion, respectively. They have been obtained for 21 energies between 1 and 300 keV by fitting the analytical function $f(z)$ to Monte Carlo results. The parameters as a function of energy have in turn been fitted by the following formula:

$$a_i = \begin{cases} a \cdot E + b \cdot E^2 + c \cdot E^3, & E \le E_0 \\ d \cdot E^p + e, & E \ge E_0 \end{cases} \tag{9}$$

a_i represents a_1, a_2, a_3, or N_{vac}. b, c, d, p, and E_0 are listed in Tables I-IV, a and e are calculated from continuity and continuity of the first derivative in E_0:

$$a = d \cdot p \cdot E_0^{p-1} - 2 \cdot b \cdot E_0 - 3 \cdot c \cdot E_0^2 \tag{10a}$$

$$e = a \cdot E_0 + b \cdot E_0^2 + c \cdot E_0^3 - d \cdot E_0^p. \tag{10b}$$

The units for lengths are angstroms, the units for energy kiloelectronvolts. A single Gaussian function is to be used

TABLE I
DECAY LENGTH a_1

	B	P	As	Sb
b	1.21	0.174	0.0833	0.808
c	−0.0161	0.00213	0.00051	−0.0435
d	7850	188	−14.5	−6.54
p	0.0852	0.571	0.529	0.660
E_0	47.7	44.2	7.34	9.10

TABLE II
PEAK POSITION a_2

	B	P	As	Sb
b	0.166	−0.131	−2.40	−2.68
c	−0.00118	0.00148	0.153	0.176
d	219	8.97	4.75	4.48
p	0.643	1.04	0.971	0.913
E_0	77.9	56.9	5.21	5.01

TABLE III
STANDARD DEVIATION a_3

	B	P	As	Sb
b	−0.395	−0.372	−0.931	−1.93
c	0.00251	0.00710	0.0448	0.147
d	92.58	414	3.14	3.06
p	0.272	0.217	0.985	0.917
E_0	51.2	27.2	6.89	4.34

TABLE IV
NUMBER OF VACANCIES PER ION N_{vac}

	B	P	As	Sb
b	−0.341	−0.169	−0.0489	−0.0560
c	0.00270	0.00083	−0.00033	0.00020
d	130	418	52.9	58.8
p	0.307	0.364	0.765	0.768
E_0	38.6	74.6	28.2	46.8

used for boron at energies $E < 20$ keV, phosphorus at $E < 55$ keV, and arsenic at $E > 170$ keV. In these cases a_1 must be ignored.

The root mean square error for fitting a_1, a_2, a_3, and N_{vac} is about 1 percent. But it is not clear, if this error is due to bad approximation or to fluctuations in the Monte Carlo results. The quality of the analytical model is demonstrated in Figs. 7 and 8. In Fig. 7 the analytical distribution function for a boron implantation at 100 keV is compared with the corresponding Monte Carlo results. In Fig. 8 this is done for an arsenic implantation at 100 keV.

3.2. Two-Dimensional Model

Two-dimensional distributions may be constructed from point responses [21], [22] for dopant profiles as well as for damage profiles. So we will deal in this section only with point responses.

A natural way of extending the moments method to the two-dimensional case is to construct the distribution function from vertical, lateral, and cross moments. The cross moments describe the correlation between the vertical and the lateral profile. Such a model has recently been presented by Winterbon [23], however, the results are not fully convincing.

We have previously presented another model, which is based on the concept of depth dependent lateral moments [17]. Apart from a summary of this model, we show here that it applies well to damage distributions, and we give tables for the parameters. The model in its general form

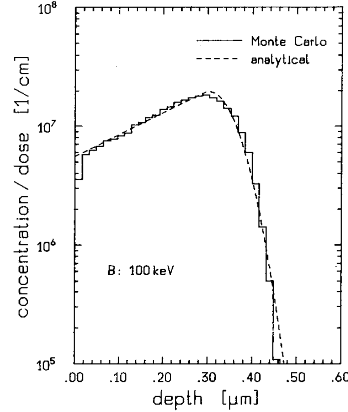

Fig. 7. Comparison of the analytical model (dashed line) with the underlying Monte Carlo results (full line) for a boron implantation at 100 keV.

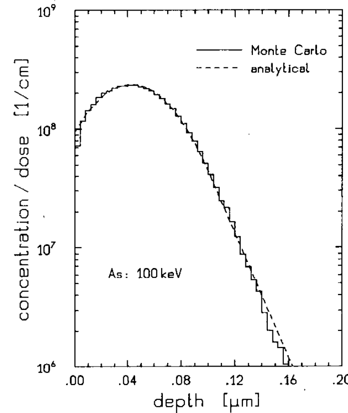

Fig. 8. Comparison of the analytical model (dashed line) with the underlying Monte Carlo results (full line) for an arsenic implantation at 100 keV.

reads

$$f(z, x) = f_{vert}(z) \cdot f_{lat}(x, z) \tag{11}$$

with

$$\int_{-\infty}^{+\infty} f_{lat}(x, z)\, dx = 1. \tag{12}$$

The point response $f(z, x)$ is obtained by multiplying the vertical distribution function $f_{vert}(z)$, e.g. as obtained from Section 3.1, with a lateral distribution function $f_{lat}(x, z)$, which depends on the depth. The depth dependence of f_{lat} is introduced by the depth dependence of the lateral moments. Take for instance a Gaussian function:

$$\text{gauss}(x) = \frac{1}{\sqrt{2\pi} \cdot \sigma_x} \cdot \exp\left(-\frac{x^2}{2 \cdot \sigma_x^2}\right). \tag{13}$$

If we allow the standard deviation σ_x to vary with z, the whole lateral distribution function will depend on z. The advantage of this model is that we need not care about the depth dependence of the lateral moments when we derive

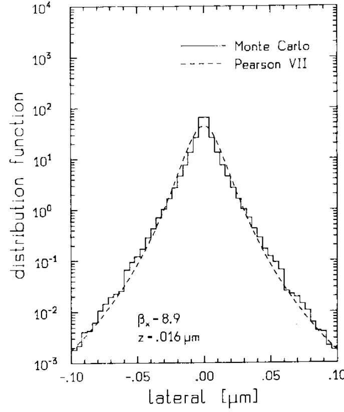

Fig. 9. Lateral profile of a point response to a 100-keV arsenic beam at a depth of 0.016 μm. Full line: Monte Carlo results, dashed line: analytical model.

formulas for the calculation of the parameters of the distribution function.

There are two tasks to do in this model: First, one has to construct a lateral distribution function from the lateral moments. In the simplest case this is done by constructing a Gaussian function from its standard deviation. In Fig. 9 an example for the lateral distribution function near the surface is shown. One can see that it is not well represented by a Gaussian function, since a Gaussian function would appear as a parabola in this representation. So it is desirable to take higher moments into account. To include the lateral kurtosis β_x, we propose a modified Gaussian function for $\beta_x \leq 3$,

$$f(x) = a \cdot \exp\left(-|b \cdot x|^p\right) \tag{14}$$

and a Pearson VII function for $\beta_x > 3$

$$f(x) = C \cdot \left|1 + \frac{b_2}{b_0} \cdot x^2\right|^{1/2b_2}. \tag{15}$$

The calculation of the parameters a, b, p, and C, b_0, b_2, respectively, from σ_x and β_x is straightforward (for details, see [17]). In Fig. 9 the Monte Carlo results are compared with a Pearson VII function and the agreement is very good.

The second task is to specify lateral moments as a function of depth and favorably as a function of implantation energy. We do this by the following formulas:

$$\sigma_x(z, E) = \sigma_z(E) \cdot \left[\frac{1}{a_1} \cdot \ln\left(e^{a_1 \cdot P_1} + e^{a_1 \cdot P_2}\right)\right] \tag{16a}$$

$$\beta_x(z, E) = \frac{1}{a_1} \cdot \ln\left(e^{a_1 \cdot P_1} + e^{a_1 \cdot P_2}\right) \tag{16b}$$

with

$$P_1 = a_2 \cdot z' \cdot E + a_3 \cdot z' + a_4 \cdot E + a_5 \tag{17a}$$

$$P_2 = a_6 \cdot z' \cdot E + a_7 \cdot z' + a_8 \cdot E + a_9 \tag{17b}$$

TABLE V
LATERAL STANDARD DEVIATION σ_x

	B	P	As	Sb
a_1	−7.839	−8.747	23.28	$1.3 \cdot 10^6$
a_2	−0.0003591	−0.0001638	−0.0004465	0.0000649
a_3	0.5335	0.4631	0.2955	0.2298
a_4	−0.0006606	−0.0004085	−0.001393	−0.0004593
a_5	0.2204	0.2163	0.3659	0.3869
a_6	−0.005708	−0.001238	−0.0002071	0.0001246
a_7	0.004471	0.09083	0.3434	0.3328
a_8	0.006822	0.001224	0.0000031	−0.0004846
a_9	0.9171	0.7157	0.2197	0.2369

TABLE VI
LATERAL KURTOSIS β_x

	B	P	As	Sb
a_1	0.03991	0.02170	0.01408	0.005920
a_2	−0.1492	−0.03615	−0.2277	−0.1892
a_3	−96.65	−127.8	−191.4	−482.3
a_4	0.2045	0.1218	0.2133	0.4105
a_5	23.60	−55.71	−136.4	−533.2
a_6	−0.003087	−0.000510	−0.002097	−0.002816
a_7	−0.09187	−0.2583	−0.6595	−0.9645
a_8	0.003051	−0.000539	0.004463	0.007533
a_9	3.059	3.643	5.258	6.276

TABLE VII
PROJECTED RANGE R_p

	B	P	As	Sb
a_1	55.00	11.39	6.14	5.25
a_2	0.8142	0.9479	0.9419	0.9038
a_3	−70.56	18.47	23.45	24.00

TABLE VIII
STANDARD DEVIATION σ_z

	B	P	As	Sb
a_1	52.11	8.848	4.016	3.221
a_2	0.6580	0.8635	0.9100	0.8880
a_3	−79.33	0.94	9.532	9.98

and z' the reduced depth

$$z' = \frac{z}{R_p(E)}. \tag{17c}$$

The parameters a_1–a_9 have been fitted to the Monte Carlo results and are given in Tables V and VI.

R_p in (17c) denotes the mean range and σ_z in (16a) the mean standard deviation of the vertical damage profile. They have been fitted by

$$R_p(E) = a_1 \cdot E^{a_2} + a_3 \tag{18a}$$

$$\sigma_z(E) = a_1 \cdot E^{a_2} + a_3. \tag{18b}$$

a_1–a_3 are found in Tables VII and VIII.

R_p and σ_z are given in angstroms. To obtain them in micrometers, divide by 10^4. Note that in all formulas energies must be inserted in kiloelectronvolts. Furthermore, to avoid numerical problems, it might be necessary to truncate σ_x and β_x at, e.g., $\sigma_x = \sigma_z/100$ and $\beta_x = 2$. This truncation has no physical meaning as it operates only for large z where the vertical profile is already negligibly small. The two-dimensional model is intended to be applied only to energies between 10 and 300 keV.

Finally, we give an example of a comparison of our analytical model with the underlying Monte Carlo results. Fig. 10 shows good agreement between the two distributions.

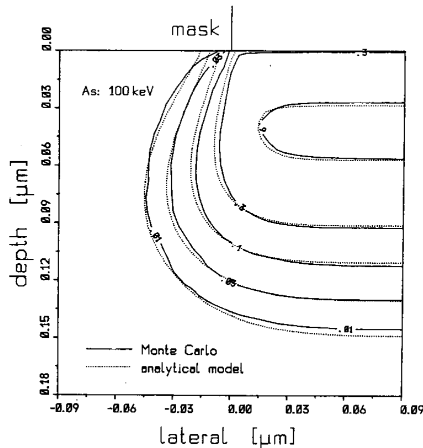

Fig. 10. Comparison of the two-dimensional analytical model (dotted lines) with the underlying Monte Carlo results (full lines). Arsenic implanted into silicon by a vertical mask edge at 100 keV.

Acknowledgment

We are indebted to Professor H. Pötzl for carefully reading the manuscript and to E. Guerrero for many helpful discussions.

References

[1] D. A. Antoniadis, "Oxidation-induced point defects in silicon," *J. Electrochem. Soc.*, vol. 129, no. 5, pp. 1093-1097, 1982.

[2] D. Collard and K. Taniguchi, "IMPACT—A point-defect-based two-dimensional process simulator: Modeling the lateral oxidation-enhanced diffusion of dopants in silicon," *IEEE Trans. Electron Dev.*, vol. ED-33, pp. 1454-1462, 1986.

[3] J. D. Plummer *et al.*, "Process simulators for silicon VLSI and high speed GaAs devices," Integrated Circuits Lab. Stanford Univ., Stanford, CA, July 1986.

[4] K. Cho, M. Numan, T. G. Finstad, W. K. Chu, J. Liu, and J. J. Wortman, "Transient enhanced diffusion during rapid thermal annealing of boron implanted silicon," *Appl. Phys. Lett.*, vol. 47, no. 12, pp. 1321-1323, 1985.

[5] T. E. Seidel, D. J. Lischner, C. S. Pai, R. V. Knoell, D. M. Maher, and D. C. Jacobson, "A review of rapid thermal annealing (RTA) of B, BF_2 and As ions implanted into silicon," *Nucl. Instr. Meth.*, vol. B 7/8, pp. 251-260, 1985.

[6] K. B. Winterbon, *Ion Implantation Range and Energy Deposition Distributions*. vol. 2. New York: Plenum, 1975.

[7] H. Matsumura and S. Furukawa: "Lateral spread of damage formed by ion implantation," *J. Appl. Phys.*, vol. 47, no. 5, pp. 1746-1751, 1976.

[8] L. A. Christel, J. F. Gibbons, and S. Mylroie, "An application of the Boltzmann transport equation to ion range and damage distributions in multilayered targets," *J. Appl. Phys.*, vol. 51, no. 12, pp. 6176-6182, 1980.

[9] M. T. Robinson and I. M. Torrens, "Computer simulation of atomic-displacement cascades in solids in the binary-collision approximation," *Phys. Rev.*, vol. B 9, no. 12, pp. 5008-5024, 1974.

[10] M. Posselt and J. P. Biersack, "Influence of recoil transport on energy-loss and damage profiles," *Nucl. Instr. Meth.*, vol. B 15, pp. 20-24, 1986.

[11] D. A. Thompson, A. Golanski, K. H. Haugen, D. V. Stevanovic, G. Carter, and C. E. Christodoulides, "Disorder production and amorphisation in ion implanted silicon," *Rad. Eff.*, vol. 52, pp. 69-84, 1980.

[12] D. A. Thompson and R. S. Walker, "Energy Spikes in Si and Ge due to Heavy Ion bombardment," *Rad. Eff.*, vol. 36, pp. 91-100, 1978.

[13] C. Prunier, E. Ligeon, A. Bourret, A. C. Chami, and J. C. Oberlin, "Defects created by self-implantation in Si as a function of temperature and fluence," *Nucl. Instr. Meth.*, vol. B 17, pp. 227-233, 1986.

[14] E. F. Krimmel, H. Oppolzer, and H. Runge, "Transmission electron microscopical imaging of lateral implantation effects near mask edges in B^+-implanted Si wafers," *Rev. Phys. Appl.*, vol. 13, pp. 791-795, Dec. 1978.

[15] A. M. Mazzone, "Three-dimensional Monte Carlo simulations—Part II: Recoil phenomena," *IEEE Trans. Computer-Aided Design*, vol. CAD-4, pp. 110-117, 1985.

[16] J. Albers, "Monte Carlo calculation of one- and two-dimensional particle and damage distributions for ion-implanted dopants in silicon," *IEEE Trans. Computer-Aided Design*, vol. CAD-4, pp. 374-383, 1985.

[17] G. Hobler, E. Langer, and S. Selberherr, "Two-dimensional modeling of ion implantation with spatial moments," *Solid-State Electron.*, vol. 30, no. 4, pp. 445-455, 1987.

[18] G. H. Kinchin and R. S. Pease, "The displacement of atoms in solids by radiation," *Rep. Prog. Phys.*, vol. 18, pp. 1-51, 1955.

[19] P. Sigmund, "A note on integral equations of the Kinchin-Pease type," *Rad. Eff.*, vol. 1, pp. 15-18, 1969.

[20] M. J. Norgett, M. T. Robinson, and I. M. Torrens, "A proposed method of calculating displacement dose rates," *Nucl. Eng. Des.*, vol. 33, pp. 50-54, 1975.

[21] S. Furukawa, H. Matsumura, and H. Ishiwara, "Theoretical considerations on lateral spread of implanted ions," *Jap. J. Appl. Phys.*, vol. 11, no. 2, pp. 134-142, 1972.

[22] H. Runge, "Distribution of implanted ions under arbitrarily shaped mask edges," *Phys. Stat. Sol.*, vol. (a) 39, pp. 595-599, 1977.

[23] K. B. Winterbon, "Calculating moments of range distributions," *Nucl. Instr. Meth.*, vol. B 17, pp. 193-202, 1986.

*

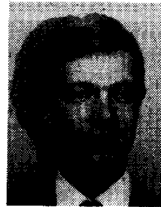

Gerhard Hobler (S'87) was born in Vienna, Austria, on July 9, 1961. He received the Diplomingenieur degree in communications engineering from the Technical University of Vienna in 1985. His master's thesis dealt with Monte Carlo simulation of ion implantation. In November 1985 he joined the Institut für Allgemeine Elektrotechnik und Elektronik, where he is working on his doctor's thesis. His dissertation is on two-dimensional process modeling and process simulation.

*

Siegfried Selberherr (M'79-SM'84) was born in Klosterneuburg, Austria, on August 3, 1955. He received the degree of Diplomingenieur in control theory and industrial electronics from the Technical University of Vienna in 1978.

Since that time he has been with the Institut für Allgemeine Elektrotechnik und Elektronik—previously called the Institut für Physikalische Elektronik—at the Technical University of Vienna as Professor. He finished his thesis, "Two Dimensional MOS-Transistor Modeling," in 1981. Dr. Selberherr has held the 'venia docendi' on Computer-Aided Design since 1984. In 1983 he received the Dr. Ernst Fehrer award; in 1985 he received the award of the Nachrichtentechnische Gesellschaft, in 1986 he was honored with the Dr. Herta Firnberg Staatspreis, and in 1987 he received the Heinz Zemanek award. His current topics are modeling and simulation of devices and circuits for application in electronic systems.

Dr. Selberherr has authored or coauthored more than 100 publications in journals and conference proceedings. Furthermore, he wrote the book *Analysis and Simulation of Semiconductor Devices*. Dr. Selberherr is a member of the Association for Computing Machinery (1979), the Society of Industrial and Applied Mathematics (1980), and the Verband deutscher Elektrotechniker (1984). He is editor of *The Transactions of the Society for Computer Simulation*, of *Electrosoft*, and of the Springer-Verlag book series Computational Microelectronics.